Reprinted from

JAPANESE JOURNAL OF
APPLIED
PHYSICS

REGULAR PAPER

Mechanisms of Local Planarization Improvement Using Solo Pad in Chemical Mechanical Polishing

Akira Isobe, Toshiyuki Yokoyama, Takashi Komiyama, and Syuhei Kurokawa

Jpn. J. Appl. Phys. **52** (2013) 126501

© 2013 The Japan Society of Applied Physics

Person-to-person distribution (up to 10 persons) by the author only. Not permitted for publication for institutional repositories or on personal Web sites.

Japanese Journal of Applied Physics **52** (2013) 126501 **REGULAR PAPER**
http://dx.doi.org/**10.7567/JJAP.52.126501**

Mechanisms of Local Planarization Improvement Using Solo Pad in Chemical Mechanical Polishing

Akira Isobe[1]*, Toshiyuki Yokoyama[2], Takashi Komiyama[2], and Syuhei Kurokawa[1]

[1] *Kyushu University, Fukuoka 819-0395, Japan*
[2] *Tokyo Seimitsu Co., Ltd., Hachioji, Tokyo 192-0032, Japan*
E-mail: iso6016@yahoo.co.jp

Received April 7, 2013; revised August 24, 2013; accepted September 2, 2013; published online November 13, 2013

The mechanism of local planarization improvement using a solo pad in chemical mechanical polishing (CMP) was investigated, and the pad surface temperature was found to be the key factor. The use of a solo pad results in better planarity than that of a stacked pad under the same process conditions. When Cu CMP evaluation was conducted at various platen temperatures, a good correlation of local planarity to pad surface temperature was confirmed regardless of the pad type. Planarity improved when the pad surface temperature was lowered, and the solo pad had a lower temperature than the stacked pad at the same platen temperature. It is considered that the solo pad has a higher heat conductance than the stacked pad, so that heat generated during polishing is transferred to the platen more easily through the solo pad than through the stacked pad. The reason for the better planarity with the lower pad surface temperature was explained by the change in pad elasticity by the temperature.
© 2013 The Japan Society of Applied Physics

1. Introduction

Chemical mechanical polishing (CMP) is a key process in LSI manufacturing and has wide spread applications such as interlayer dielectrics (ILD), shallow trench isolation (STI), tungsten (W) plug, copper (Cu) damascene, and replacement metal gate (RMG).[1–6] These applications can be categorized in two groups by planarization type: global planarization for ILD and local planarization for most of the others. Global planarization for ILD is aimed at achieving a flat surface within a lithography area,[1,7,8] typically $30 \times 30\,\text{mm}^2$, to increase the focus tolerance. There have been many studies of the global planarization mechanism and its modeling.[9–12] On the other hand, local planarization is aimed at creating special structures using the selectivity of the removal rate (RR) for different materials polished at the same time.[3–6] The degradation of local planarity such as by dishing or erosion[13–16] should be minimized to suppress the variation in transistor performance or interconnection resistance.

In CMP, a wafer is pressed on a rotating platen on which a polishing pad is placed with polishing slurry delivered.[8] RR is a function of pressure and the relative sliding speed between the wafer and the pad, which is known as Preston's equation.[17] Planarity is affected by the process conditions and consumables, i.e., polishing pad and slurry. Generally, a stacked pad is used for device CMP, which consists of a top layer of a hard polyurethane pad and a bottom layer of a soft foamed or fiber pad.[18] Global planarity is affected by the deformation of the polishing pad. Therefore, a solo pad, i.e., the top hard layer without the bottom soft layer, is known to be effective for global planarity.[19–21] The mechanism of local planarization is considered to be different from that of global planarization, but there have been some reports that a solo pad can also improve local planarity. David and coworkers reported that STI planarity is improved by applying a hard solo pad.[22,23] However, $4 \times 4\,\text{mm}^2$ chips with different pattern densities were evaluated in their studies and it seems that the global planarity factor instead of the local planarity factor is dominant in their planarity improvement.

In this study, we investigate the effect of a solo pad on the improvement in the local planarity in the Cu damascene process. The differences between the mechanisms and key factors for local and global planarizations are discussed from the results.

2. Experimental Procedure

Cu blanket wafers and patterned wafers were polished to evaluate the RR of Cu and surface topography. Two polishing pads, i.e., an IC1000™ (Nitta-Haas) solo pad and an IC1400™ (Nitta-Haas) stacked pad, which consists of IC1000 as the upper layer and a foamed pad as the lower layer, were compared. Both pads have concentric grooves (k-groove) on their surfaces. Commercially available slurry for copper CMP that contains colloidal silica abrasives was used. Three percent hydrogen peroxide (H_2O_2) was mixed into the slurry before polishing. A #100 dotted-type 4 in. diamond disc (Mitsubishi Material) was used as a pad conditioner.

ChaMP-332 (Accretech), a 300 mm CMP tool for mass production that has a three-platen two-head configuration, was used as the polishing equipment. One head can move from the right (or left) between the center platen to complete two-step polishing. The polishing head has a unique structure as shown in Fig. 1. It can apply uniform pressure on the basis of the air floating concept.[24] Because the wafer pressure and retainer ring pressure are independently controlled, a retainer ring pressure lower than the wafer pressure is realized. This can help in obtaining good within-wafer nonuniformity (WIWNU) with a hard solo pad. This machine is also equipped with an optical endpoint detector embedded in the platens. The timing at "just cleared" when Cu is completely removed and the barrier layer is exposed can be detected by monitoring the change in reflectivity. The platens have coolant paths in them and a chiller is connected to the paths to control the plate temperature. The temperature of the coolant was set to 20 °C for the first part of the evaluation and varied from 10 to 40 °C for the second part of the evaluation. An IR camera was used to evaluate the detailed temperature distribution of the pad surface.

Polishing was carried out at a wafer pressure of 20.7 kPa and a retainer ring pressure of 6.9 kPa. Slurry was supplied to a platen at a flow rate of 270 ml/min, while the platen and head were rotated at speeds of 83 and 78 min^{-1}, respec-

 © 2013 The Japan Society of Applied Physics

Person-to-person distribution (up to 10 persons) by the author only. Not permitted for publication for institutional repositories or on personal Web sites.

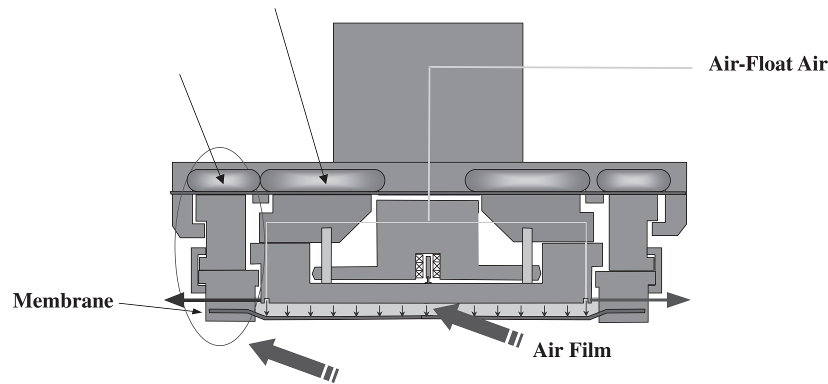

Fig. 1. Polishing head structure of ChaMP-332.

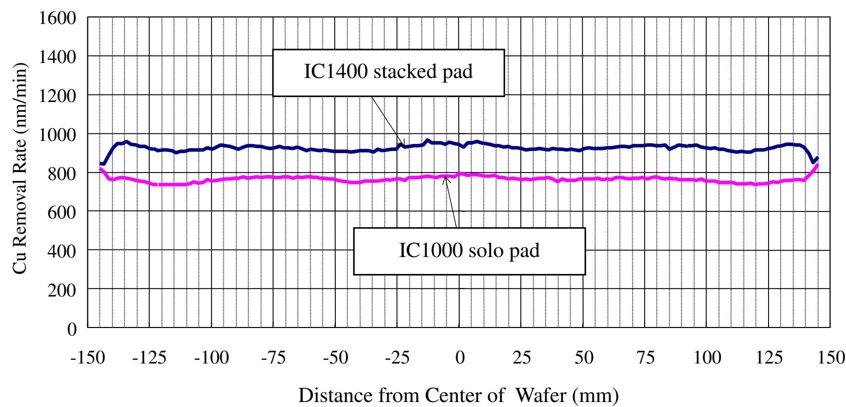

Fig. 2. (Color online) Removal rate profile for blanket Cu wafer polishing along the diameter of the wafer.

tively. The polishing pad was conditioned for 30 s in the ex-situ mode at a disc load of 59 N, a platen rotational speed of 80 min^{-1}, and a disc rotational speed of 88 min^{-1}.

The polished wafers were Cu blanket wafers with 1.5 µm Cu thickness and MIT754 patterned wafers with 1000 nm Cu thickness and 15 nm Ta thickness. The polishing time for the blanket wafers was 60 s and that for the patterned wafers was determined using the end point detection system as "just cleared".

RR was calculated by monitoring the difference in the Cu thickness before and after polishing using a four-probe metal thickness measurement system. The RR distribution along the diameter of the wafer was measured. The dishing and erosion[13–16] of the patterned wafer were evaluated with a stylus profilometer. A pattern of line/space (L/S) = 9.0 µm/1.0 µm was used to represent the local planarity. Four sites from the center to the edge in the radial direction were measured.

3. Results and Discussion

The RRs of the blanket Cu film were evaluated for an IC1400 stacked pad and an IC1000 solo pad with the platen temperature set at 20 °C. The RR profiles of all the wafers are shown in Fig. 2. The average RR of IC1400 was 925 nm/min with a nonuniformity of 1.9% (1σ), while that of IC1000 was lower at 765 nm/min with a nonuniformity of 2.0%. Then, the patterned wafers were polished under the same conditions. The average variation of topography for

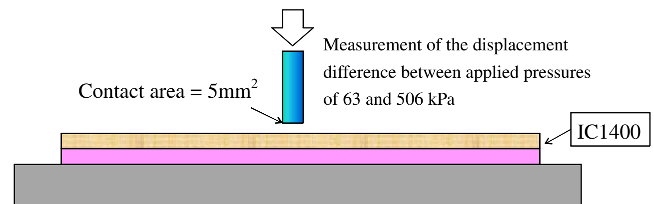

Fig. 3. (Color online) Pad compressibility measurement.

IC1400 was 72 nm and that for IC1000 was 59 nm. The IC1000 solo pad produces a lower RR and better planarity than the IC1400 stacked pad.

Both of the pads have the same layer of IC1000 on top. The only difference is the existence of a soft lower pad. When compressibility is measured as shown in Fig. 3, the IC1000 solo pad shows a compressibility of 1% or less and IC1400 shows a compressibility of 3 to 4%. This difference can explain the above result, that is, the lower compressibility of IC1000 causes better planarity as in the case of ILD planarization[19–21] and also causes a lower RR because of the less contact of the pad with the wafer due to the lower flexibility, which cannot compensate for the pad surface waviness.[25] However, as will be discussed later, the mechanism of local planarization such as STI or Cu damascene CMP must be different from that of global planarization such as that of ILD CMP, and other factors are considered to dominate the mechanism.

 © 2013 The Japan Society of Applied Physics

Person-to-person distribution (up to 10 persons) by the author only. Not permitted for publication for institutional repositories or on personal Web sites.

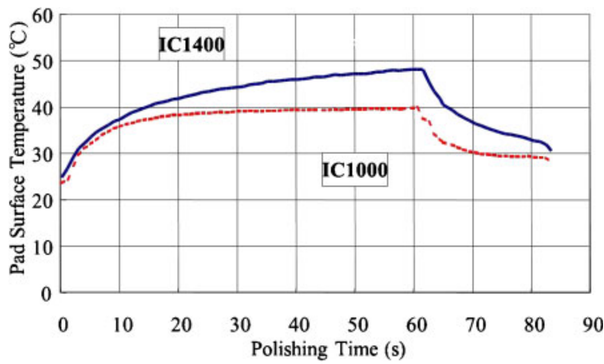

Fig. 4. (Color online) Change in pad surface temperature during polishing.

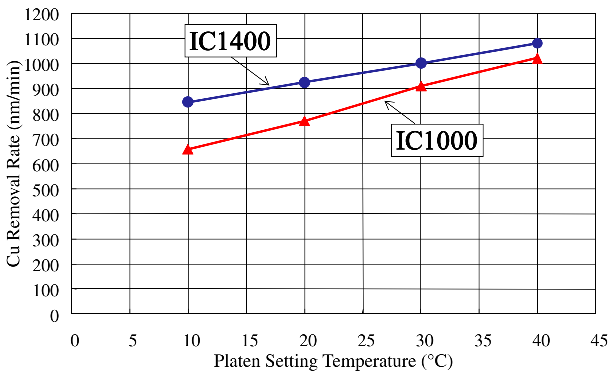

Fig. 5. (Color online) Relationship between Cu removal rate and platen setting temperature.

One possible factor is the temperature during polishing. Figure 4 shows the change in the temperature during blanket wafer polishing. Both of the pads show temperature increases but only IC1000 shows saturation at 40 °C after approximately 30 s from the start of polishing. This is considered to be due to the difference in heat conductance between the pads. IC1400 has a lower heat conductance than IC1000 because of the existence of a lower foamed pad, and heat generated during polishing cannot easily escape to the platen.

To confirm the above, a polishing test was conducted while varying the platen temperature. Figure 5 shows the relationship between the platen setting temperature and Cu RR. RR increases in both pads with increasing platen temperature but the slope for IC1400 is gentler than that for IC1000. Figure 6 shows the relationship between platen setting temperature and the amount of dishing and erosion. The trend is similar to that shown in Fig. 5.

The pad surface temperature during polishing was monitored using an IR camera. Figure 7 shows examples of the measurement where the platen setting temperature is 20 °C and the indicated temperatures are highest at the end of the polishing. Colors in the images show the temperature distribution for each point. A high temperature is observed at the polishing pad surface just behind the polishing head and the area on the pad corresponding to the wafer center showed the highest temperature. By comparing IC1400 with IC1000, a higher temperature and a wider temperature

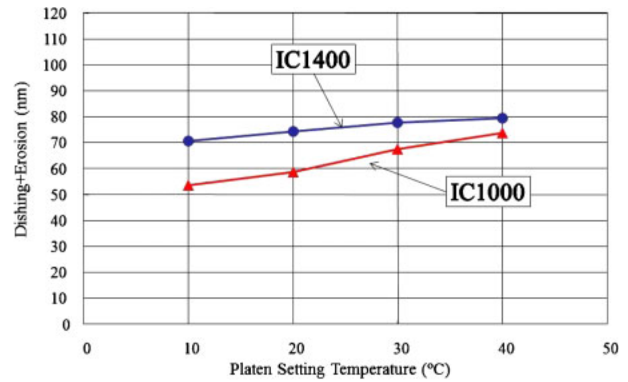

Fig. 6. (Color online) Relationship between local planarity and platen setting temperature.

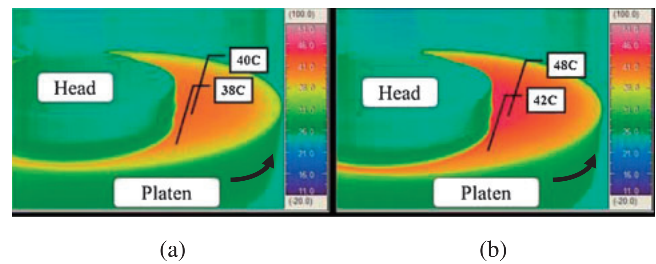

(a) (b)

Fig. 7. (Color) Thermographic views of (a) IC1000 and (b) IC1400 during polishing.

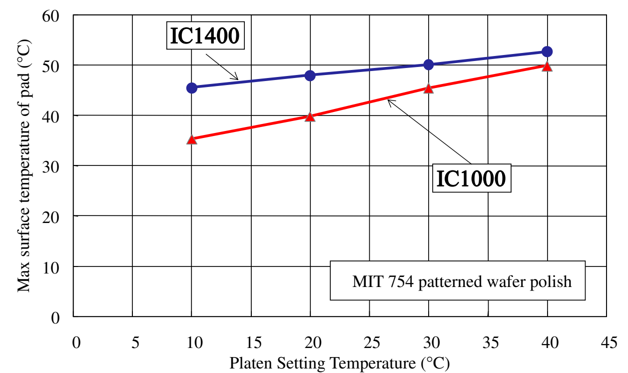

Fig. 8. (Color online) Relationship between maximum temperature of pad surface and platen setting temperature.

variation are observed in IC1400 than in IC1000. Two points corresponding to the wafer center and wafer edge on the polishing pad were chosen to precisely monitor the temperature change as shown in Fig. 7. The highest temperature during polishing was plotted in Fig. 8 with respect to the platen setting temperature. A steeper slope appears in the IC1000 solo pad than in IC1400 stacked pad, which indicates the higher heat conductivity of the IC1000 solo pad than that of the IC1400 stacked pad. To clarify the relationship between the polishing pad surface temperature and polishing performance, Figs. 5 and 6 are converted into Figs. 9 and 10, respectively, with respect to the highest pad surface temperature during polishing. These figures show good correlations of the highest pad surface temperature

 © 2013 The Japan Society of Applied Physics

Person-to-person distribution (up to 10 persons) by the author only. Not permitted for publication for institutional repositories or on personal Web sites.

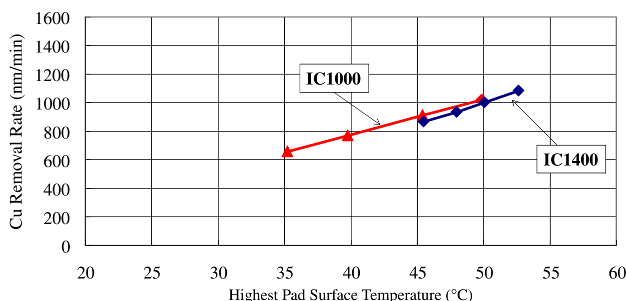

Fig. 9. (Color online) Relationship between Cu RR and maximum temperature of pad surface.

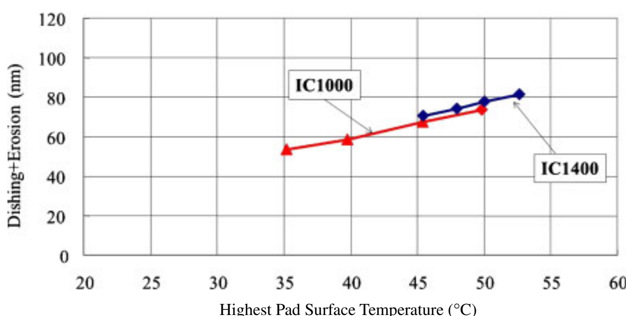

Fig. 10. (Color online) Relationship between local planarity and maximum temperature of pad surface.

to RR, as well as to the amount of dishing and erosion, regardless of the pad type.

The amount of dishing and erosion at every measurement site on the wafer is plotted in Fig. 11. The amount is lower and its variation is smaller in IC1000 than in IC1400. On the other hand, the highest amount of dishing and erosion is observed around the center of the wafer.

All the results indicate that the pad surface temperature, which is considered to be dominated by the difference in the heat conductivity between the pads, is the key factor determining RR and local planarity. Next, the mechanisms of the temperature dependencies of RR and polished pattern topography are discussed. The increase in RR in IC1400 is simply understood as the enhancement of the chemical factor caused by the heat generation in CMP. The change in topography can also be explained by the same mechanism, that is, the etching factor is enhanced by the temperature rise resulting in an increase in the amount of dishing. If this is the case, there should be no pattern size dependence of the erosion or dishing deterioration caused by a higher temperature. The amount of dishing changed by more than 30 nm for the 9.0/1.0 µm (L/S) pattern, but the dishing value itself for the isolated 1 µm line pattern was less than 5 nm under all the conditions. This result contradicts the hypothesis that the etching effect is enhanced by temperature. Another possibility is the changes in pad physical properties caused by heat. The mechanisms of global and local planarizations in relation to pad properties are considered as follows.

In the case of ILD CMP, planarization proceeds as a result of the difference in local pressure induced by the surface topography, as shown in Fig. 12. The actual polishing pad

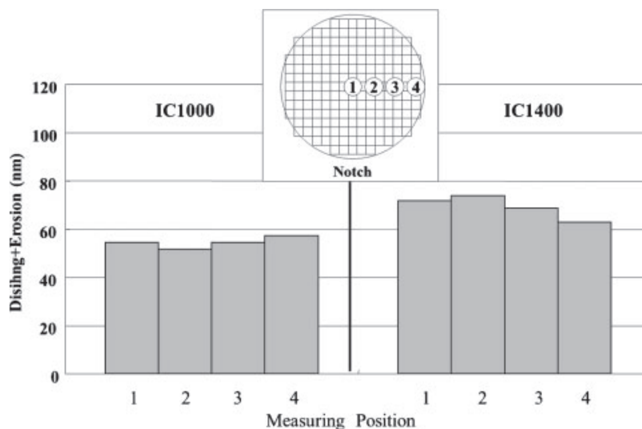

Fig. 11. Amount of dishing and erosion in wafer.

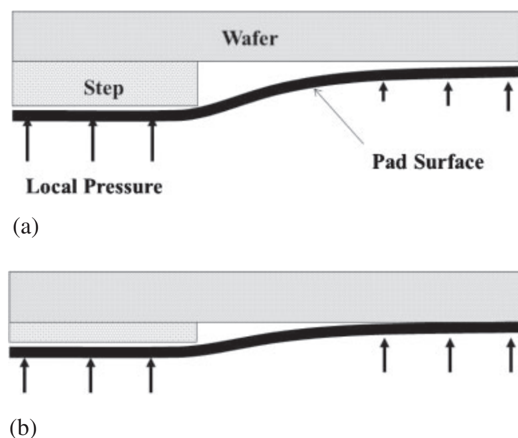

Fig. 12. Schematic diagram to explain global planarization mechanism. (a) At the start of polishing, the raised area has a higher RR because of its higher local pressure than the flat area. (b) After planarization, the difference in local pressure becomes zero and the planarization no longer proceeds.

has many pores and asperities of micrometer orders, and the percentage of the area of contact between the pad surface and the wafer is only 1% or less.[26,27] However, a model such as that shown in Fig. 12, where the pad surface is treated as a smooth surface, is considered to be reasonable as long as the macro behavior of the polishing pad is discussed. In the beginning of the polishing, the difference in the local pressure between a convex area and a concave area that have a certain distance between them, is large and the planarization speed is high, as shown in Fig. 12(a). After polishing proceeds and the step height decreases, the local pressures become the same between the convex area and the concave area, as shown in Fig. 12(b). This is the limitation of planarity, which is related to the pad deformation. If the pad deformation is small, the distance for the limit of the planarity between the convex and concave areas increases or the step height decreases. Boning et al.[10] simulated the planarity by considering the pattern density and pad deformation, calculating the planarity from the pad physical properties, i.e., Young's modulus and Poisson's ratio. When we consider the deformation of the stacked pad, the effective

 © 2013 The Japan Society of Applied Physics

Person-to-person distribution (up to 10 persons) by the author only. Not permitted for publication for institutional repositories or on personal Web sites.

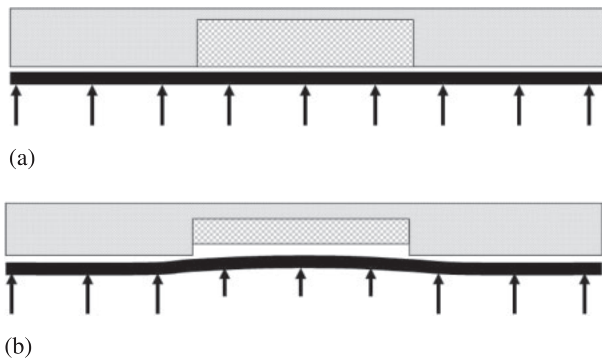

Fig. 13. Schematic diagrams to explain local planarization mechanism (1). (a) Shortly after multiple materials are exposed, there is no local pressure difference and a step is created because of the selectivity of material RRs. (b) After polishing, the created step causes a local pressure difference and the deterioration of local planarity stops when the local pressure ratio becomes the inverse of the RR selectivity. This means the RRs for both materials becomes equal if the CMP follows Preston's equation.

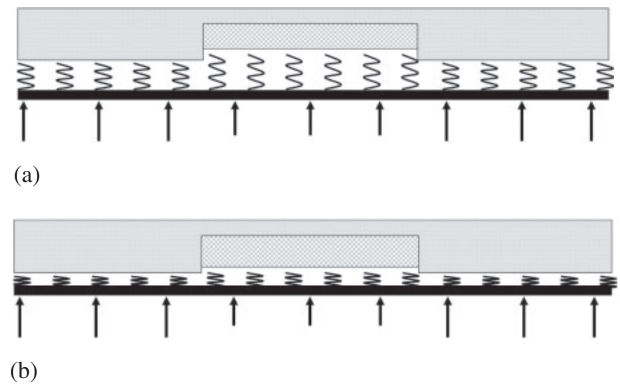

Fig. 14. Schematic diagram to explain local planarization mechanism (2). Considering the pad surface as being composed of small springs makes it easier to understand the local planarization phenomenon than considering pad bending deformation. (a) Soft springs cannot make a large difference in local pressure with small steps and cause the deterioration of the planarity. (b) Hard springs can make a large difference in local pressure with small steps and the deterioration of the local planarity to stop immediately.

parameters for the deformation are considered to be the bending modulus[28] of the top layer and the Young's modulus of the bottom layer. This seems to be very similar to the pad compressibility measurement method shown in Fig. 3. This is the mechanism of global planarization improvement using the solo pad.

On the other hand, in the case of the STI or Cu damascene process, planarization consists of two steps. The first one is to planarize the initial steps and the second one is to remove residual films on the stopper layer, such as the oxide film from the SiN layer in the case of STI or the Cu film from the barrier layer in the case of Cu CMP. The first step is similar to ILD CMP but the planarization is generally easy because the patterns have small features.

Thus, we focus on the second step where we assume that local planarization starts from a flat surface and becomes worse with polishing time. If the selectivity is 1.0, that is, if the RRs of the buried material and stopper material are the same, there will be no deterioration of planarity. In general, however, STI or Cu CMP usually uses a high-selectivity slurry between SiO_2 and Si_3N_4 for STI, and Cu and a barrier for Cu CMP. For example, provided that the Cu RR is 10 times higher than the Ta RR, the RRs of these materials are the same for blanket wafers when Cu is just cleared because of the lack of the difference in pressure, as shown in Fig. 13(a). Then, the local step height increases because of the difference between the RRs. At the same time, the pressure difference increases because of the generated steps. If the RR follows Preston's formula, the local step height increases until the pressure difference ratio becomes 1 to 10, as shown in Fig. 13(b).

If we consider the pad surface to be smooth and flat, the pressure difference increases rapidly at such micrometer scale features even with a very small step, and the deterioration of local planarity stops immediately. Thus, the mechanism of local planarization should be different from that of global planarization and we should not consider the pad surface to be smooth and flat. Elbel et al. proposed a model of a spring network for tungsten dishing[29] and Vlassak reported the relationship between pad asperity and dishing.[13] The spring model shown in Fig. 14 makes it is easy to understand the local planarization. When the spring constant is large, i.e., the effective surface elasticity is high, the pressure difference increased and the local planarity deterioration stops immediately. On the other hand, when the spring constant is small, i.e., the surface elasticity is low, the pressure difference cannot increase even after the step height increases. The effective elasticity of the pad is considered to be a function of surface asperity and material elasticity.

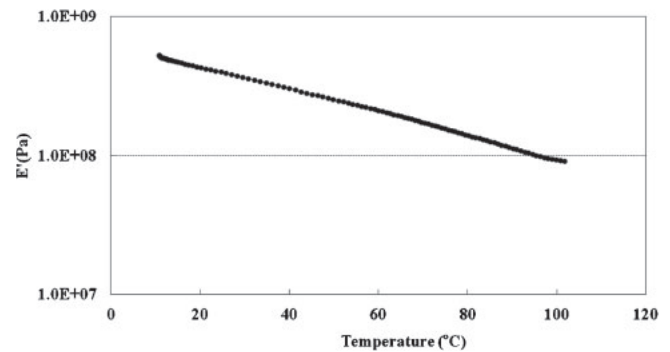

Fig. 15. Temperature dependence of elasticity (E') for IC1000.

The bulk elasticity measurement of a polishing pad by dynamic mechanical analysis was reported,[30,31] and the temperature dependence of elasticity (E') for IC1000, as shown in Fig. 15, is widely recognized. The elasticity decreases with increasing temperature. The mechanism of local planarization improvement by the solo pad is explained by this pad elasticity trend, however, bulk elasticity is not the key factor. Bulk elasticity must have a strong correlation to the effective surface elasticity, and the change in the effective surface elasticity is considered to explain the results of this study.

The solo-pad can maintain a low surface temperature and a high effective surface elasticity during polishing to improve local planarity. Using the CMP tools used in this

 © 2013 The Japan Society of Applied Physics

Person-to-person distribution (up to 10 persons) by the author only. Not permitted for publication for institutional repositories or on personal Web sites.

study, which can be applied to a solo pad, is one approach to local planarity improvement. Another approach is to control the effective pad surface elasticity from the viewpoints of material elasticity and pad surface asperity. This provides a clue to pad material and pad conditioning development. The direct measurement of effective pad surface elasticity[32] will be a key technology and another challenge for the development of pad material and pad conditioning to improve local planarity.

4. Conclusions

Copper damascene CMP using a solo pad improves planarity as in the case of ILD CMP, compared with that using a stacked pad. However, the planarization mechanism of Cu CMP is different from that of ILD CMP. It is considered that the higher heat conductivity of the IC1000 solo pad could keep the pad surface temperature low and the elasticity high to prevent dishing enhancement. This result indicates that there is room to improve local planarity by keeping the effective pad surface elasticity high. A method for evaluating the effective pad surface elasticity separately from the bulk property will be a key technology for the development of pad materials and pad conditioning to improve local planarity.

Acknowledgement

The authors would like to thank Ms. Kawai of Nitta Haas for providing the pad DMA data.

1) A. Isobe: Proc. SEMI Technology Symp. Japan, 1991, p. 276.
2) M. Krishnan, J. W. Nalaskowski, and L. M. Cook: Chem. Rev. **110** (2010) 178.
3) Y. Moon, R. Venigalla, C. Sheraw, C. Wang, J. Cummings, D. Canaperi, D. Lee, L. Hall, and L. Economikos: Proc. ICPT, 2009, p. 183.
4) K. Wijekoon, R. Lin, B. Flankin, S. Yang, F. Redeker, G. Amico, and S. Nanjangud: Solid State Technol. **22** (1998) 53.
5) S.-Y. Kim and Y.-J. Seo: Microelectron. Eng. **60** (2002) 357.
6) H.-P. Feng, J.-Y. Lin, M.-Y. Cheng, Y.-Y. Wang, and C.-C. Wan: J. Electrochem. Soc. **155** (2008) H21.
7) International Technology Roadmap for Semiconductors: 2011 ed., Lithography, p. 7.
8) P. B. Zantye, A. Kumar, and A. K. Sikder: Mater. Sci. Eng. R **45** (2004) 89.
9) G. Nanz and L. E. Camilletti: IEEE Trans. Semicond. Manuf. **8** (1995) 382.
10) D. Boning, B. Lee, C. Oji, D. Ouma, T. Park, T. Smith, and T. Tugbawa: MRS Proc. **566** (1999) 197.
11) D. O. Ouma, D. S. Boning, J. E. Chung, W. G. Easter, V. Saxena, S. Misra, and A. Crevasse: IEEE Trans. Semicond. Manuf. **15** (2002) 232.
12) D. G. Thakurta, D. W. Schwendeman, R. J. Gutmann, S. Shankar, L. Jiang, and W. N. Gill: Thin Solid Films **414** (2002) 78.
13) J. J. Vlassak: MRS Proc. **671** (2001) M4.6.1.
14) S. Takemiya, N. Nakazwa, and S. Shinmaru: Rep-Res. Lab. Asahi Glass Co., Ltd. **36** (2006) 29.
15) Z. Junxiong, C. Lan, R. Wenbiao, L. Zhigang, S. Weixiang, and Y. Tianchun: J. Semicond. **31** (2010) 106003.
16) J. Warnock: J. Electrochem. Soc. **138** (1991) 2398.
17) F. Preston: J. Soc. Glass Technol. **11** (1927) 127.
18) P. Wrschka, J. Hernandez, G. S. Oehrlein, and J. King: J. Electrochem. Soc. **147** (2000) 706.
19) K. S. Choi, C. W. Nam, C. W. Jeon, C. K. Oh, M. S. Chae, S. D. Kim, and C. T. Kim: Proc. Advanced Metallization Conf., 1998, p. 225.
20) Y. Yamada, T. Sugaya, N. Konishi, S. Kurokawa, and T. Doi: Seimitsu Kogaku Kaishi **74** (2008) 1199 [in Japanese].
21) K. S. Choi, C. W. Nam, C. W. Jeon, C. K. Oh, M. S. Chae, S. D. Kim, and C. T. Kim: Proc. ULSI XIV, MRS, 1999, p. 225.
22) J. David, B. Bonner, T. Osterheld, and R. Jin: Proc. SEMI Technology Symp. in Japan, 1999, p. 8.
23) R. Jin, J. David, B. Abbassi, T. Osterheld, and F. Redeker: Proc. 4th Int. Conf. on CMP, 1999, p. 314.
24) A. Isobe, A. Yamane, K. Tanaka, S. Yamada, and M. Numoto: Proc. 8th Int. Conf. on CMP, 2003, p. 509.
25) H. J. Kim, J. K. Choi, M. K. Hong, K. Lee, and Y. Ko: ECS J. Solid State Sci. Technol. **1** (2012) P204.
26) M. Mitsuhashi, H. Ono, and A. Isobe: Proc. JSPE Fall Meet., 1995, p. 20 [in Japanese].
27) M. Akaji, S. Haba, K. Yoshida, A. Isobe, and M. Kinoshita: Proc. International Conf. Planarization/CMP Technol., 2009, p. 97.
28) ISO178:2010.
29) N. Elbel, B. Neureither, B. Ebersberger, and P. Lahnor: J. Electrochem. Soc. **145** (1998) 1659.
30) H. Lu, Y. Obeng, and K. A. Richardson: Mater. Charact. **49** (2002) 177.
31) I. Li, K. M. Forsthoefel, K. A. Richardson, Y. S. Obeng, W. G. Easter, and A. Maury: MRS Proc. **613** (2000) E7.3.
32) N. Suzuki, M. Asaba, Y. Hashimoto, and E. Shamoto: Proc. JSPE Fall Meet., 2011, p. 161 [in Japanese].

© 2013 The Japan Society of Applied Physics